

# Photon Production at the LHC

R. Lafaye

► **To cite this version:**

R. Lafaye. Photon Production at the LHC. XLVIIIth Rencontres de Moriond - QCD and High Energy Interactions, Mar 2013, La Thuile, Italy. in2p3-00815889

**HAL Id: in2p3-00815889**

**<http://hal.in2p3.fr/in2p3-00815889>**

Submitted on 21 Nov 2013

**HAL** is a multi-disciplinary open access archive for the deposit and dissemination of scientific research documents, whether they are published or not. The documents may come from teaching and research institutions in France or abroad, or from public or private research centers.

L'archive ouverte pluridisciplinaire **HAL**, est destinée au dépôt et à la diffusion de documents scientifiques de niveau recherche, publiés ou non, émanant des établissements d'enseignement et de recherche français ou étrangers, des laboratoires publics ou privés.

# PHOTON PRODUCTION AT THE LHC

R. LAFAYE, On behalf of the ATLAS and CMS collaborations  
*Laboratoire d'Annecy-le-Vieux de Physique des Particules, 9 chemin de Bellevue  
74941 Annecy-le-Vieux, France*

We review the latest results on photon production at the LHC by the ATLAS and CMS experiments obtained in proton-proton collisions with a center of mass energy of 7 TeV in 2010 and 2011, corresponding to a maximum integrated luminosity of  $5 \text{ fb}^{-1}$ . We compare the prompt photon and photon-jet differential cross sections to theoretical predictions and discuss their impact on the parton distribution functions of the proton. Di-photon differential cross sections are also presented as a function of the di-photon invariant mass, transverse momentum, azimuthal separation, and  $\cos\theta^*$ .

## 1 Introduction

Photon production measurements at hadron colliders allow precise tests of perturbative QCD predictions by providing a colorless probe of the hard scattering process<sup>1</sup>. Since the photon originates directly from the hard interaction and does not undergo hadronization the environment tends to be cleaner than for jet production. These measurements can help to probe the gluon content of the proton<sup>2</sup> as the prompt photon and photon-jet production is dominated by quark-gluon fusion. In addition, isolated prompt photon production is the main background to searches for new phenomena involving photons in the final state, most notably the Higgs boson production via the  $H \rightarrow \gamma\gamma$  mechanism.

At the Large Hadron Collider<sup>3</sup> (LHC), a significant increase of center-of-mass energy with respect to previous collider experiments allows for the exploration of new kinematic regions in the hard scattering processes in hadron-hadron collisions. The photons considered in the analyses presented in this paper include all photons produced in p-p collisions, not originating from secondary hadron decays. Isolated prompt photons are produced mainly through  $qg$  Compton scattering,  $q\bar{q}$  annihilation, and in the fragmentation of partons with large transverse momentum. For di-photons the production is dominated by the  $q\bar{q}$  annihilation, the  $gg$  fusion and the fragmentation of partons in association with a prompt photon.

Both the ATLAS<sup>4</sup> and CMS<sup>5</sup> Collaborations have performed measurements of the differential cross section of isolated prompt photon, photon-jet and di-photon production with data collected in 2010 and 2011. In this article we present the latest results from both experiments and compare them with theoretical predictions from fixed order calculations and parton shower simulations.

## 2 Photon reconstruction and signal extraction

The photon energy and position are reconstructed from the clusters in the electromagnetic calorimeter. In the case of converted photons, clusters can then be associated to one or two tracks. After cluster reconstruction, the main background comes from the decay of neutral

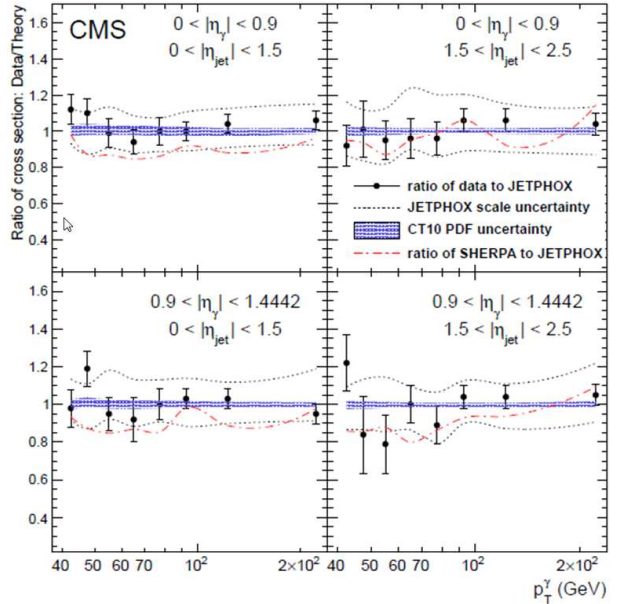


Figure 1: **Left:** Measured (dots with error bars) and expected inclusive prompt photon cross section in the ATLAS barrel  $\eta$  region<sup>10</sup>. The inner error bars on the data points show statistical uncertainties, while the full error bars show statistical and systematic uncertainties added in quadrature. The next to leading order theory prediction is shown as a shaded band which indicates theoretical uncertainties, while the leading order parton shower Monte Carlo generators are shown as lines. **Right:** The ratios of the photon-jet triple-differential cross section to the NLO QCD prediction using JETPHOX with the CT10 PDF set and scales, as measured by CMS<sup>16</sup> with  $2.14 \text{ fb}^{-1}$ . Errors show the statistical and systematic uncertainties added in quadrature. The two dotted lines represent the effect of varying the theoretical scales. The shaded region is the CT10 PDF uncertainty. The dash-dotted lines show the ratios of the SHERPA predictions to JETPHOX.

hadrons, such as  $\pi^0$  mesons, into nearly collinear pairs of photons. This jet background contamination can be estimated using discriminating criteria, such as the profile of the electromagnetic shower (identification) and the amount of energy surrounding the photon candidate (isolation).

For photon identification, ATLAS defines shower profile variables in the different layers of its calorimeters while CMS uses a topological fit of the cluster shape. Photons are considered isolated if the extra transverse energy within a cone of radius  $\Delta R = 0.4$  in  $\eta \times \phi$  ( $\eta$  is the pseudorapidity along the  $z$  axis and  $\phi$  is the azimuthal angle) centered around the photon, is lower than typically a few GeV.

The signal is then extracted using a sideband technique in the identification-isolation plane or with a template fit of the isolation profile. In both cases, efficiencies and profiles are taken from Monte Carlo generators for the photon signal and extracted using data-driven approaches for the jet background.

### 3 Isolated prompt photon production

The production cross section of isolated prompt photons is measured as a function of the transverse energy of the photon ( $E_T$ ). ATLAS measurements in 2010, with  $0.88 \text{ pb}^{-1}$ , start as low as  $10 \text{ GeV}$ ,<sup>6</sup> while ATLAS and CMS results, with  $35 \text{ pb}^{-1}$ , use  $50$  and  $25 \text{ GeV}$  cuts, respectively, due to the single photon trigger thresholds<sup>8,7</sup>. The most recent results from ATLAS cover the kinematic range  $100 \leq E_T^\gamma \leq 1000 \text{ GeV}$  and uses the 2011 data set, corresponding to an integrated luminosity of  $4.71 \text{ fb}^{-1}$ .

ATLAS and CMS results have been compared to next-to-leading order (NLO) calculations from JETPHOX<sup>11</sup> and to parton shower Monte Carlo generator predictions from PYTHIA<sup>12</sup> and HERWIG,<sup>13</sup> see figure 1 left. The highest disagreements are at low  $E_T$  values, while above

100 GeV the data is systematically higher than the predictions. At very high  $E_T$  (above 700 GeV) the prediction uncertainties are dominated by the poorly determined gluon density.

#### 4 Isolated photon plus jet production

The differential cross sections for isolated photons in association with jets are measured as functions of the photon transverse energy in different regions of rapidity of the photon (and of the leading jet for the CMS study). The chosen regions differ by the accessible  $x$  values and the amount of the fragmentation component. ATLAS performed this measurement using  $35 \text{ pb}^{-1}$  from the 2010 data set<sup>14</sup>. While newer CMS results use  $2.14 \text{ fb}^{-1}$  from the 2011 data set<sup>16</sup>, see right plot of figure 1. Recently ATLAS extended the study by measuring also cross sections in terms of other kinematic properties of the photon-jet system<sup>15</sup>: the leading-jet transverse momentum and rapidity, the difference in azimuthal angle between the photon and the jet, the photon-jet invariant mass and the cosine of the longitudinal angle difference.

The obtained distributions have been compared to JETPHOX, PYTHIA and SHERPA<sup>17</sup> predictions, and using different PDFs. The worst agreement is found for high jet rapidities but still within uncertainties. The ATLAS 2010 results use a low trigger threshold allowing to scan the  $E_T$  range down to 25 GeV. In this low  $E_T$  region, as in the single photon studies, JETPHOX overestimates the data.

#### 5 Isolated di-photon production

The differential cross section of di-photon production was measured as a function of four kinematic variables: the invariant mass and transverse momentum of the di-photon system, the azimuthal separation between the two photons, and  $\cos\theta^*$ . The first one is of obvious interest for resonance searches, while the second and the third provide important information in the study of higher order QCD perturbation and fragmentation. ATLAS defines  $\cos\theta^*$  as the cosine of the polar angle of the highest transverse momentum photon in the Collins-Soper di-photon rest frame<sup>18</sup>. CMS makes use of the rapidity difference:  $\cos\theta^* = \tanh|\Delta y_{\gamma\gamma}|/2$ . Both definitions are useful to investigate the spin of di-photon resonances.

The analyzed data set used by CMS consists of the 7 TeV p-p collisions recorded in the year 2010,<sup>19</sup> for an integrated luminosity of  $36 \text{ pb}^{-1}$ . ATLAS recently updated their results<sup>20</sup> with the data sample collected in 2011, corresponding to  $4.9 \text{ fb}^{-1}$  of integrated luminosity. The signal extraction method is the same as for single photon analyzes, extended to two photons. The largest background comes from jets decaying into neutral hadrons and is estimated as in the single photon analyses. The second main background comes from Drell-Yan events and is subtracted using electron to photon fake rates extracted from  $Z \rightarrow ee$  and  $Z \rightarrow ee\gamma$  events for the 2011 analysis. For the 2010 analysis where the statistics is too low, Monte Carlo simulated events are used.

The differential distribution obtained are compared to fixed order calculations from DIPHOX<sup>21</sup> and  $2\gamma\text{NNLO}$ ,<sup>22</sup> and parton shower Monte Carlo generators PYTHIA and SHERPA, see figure 2. The Monte Carlo generators are rescaled to correspond to the measured integrated cross section, and are in good agreement. Except for large  $\cos\theta^*$  values where all predictions tend to underestimate the data. At low  $E_T$  (and  $\Delta\phi \simeq \pi$ ) the fixed-order calculations do not reproduce the data, due to the known infrared divergences from initial-state soft gluon radiation. Everywhere else DIPHOX is missing NNLO contributions and clearly underestimates the data. Thanks to the inclusion of NNLO terms,  $2\gamma\text{NNLO}$  is able to match the data very closely within the uncertainties, except in limited regions where the neglected fragmentation component is still significant after photon isolation requirements.

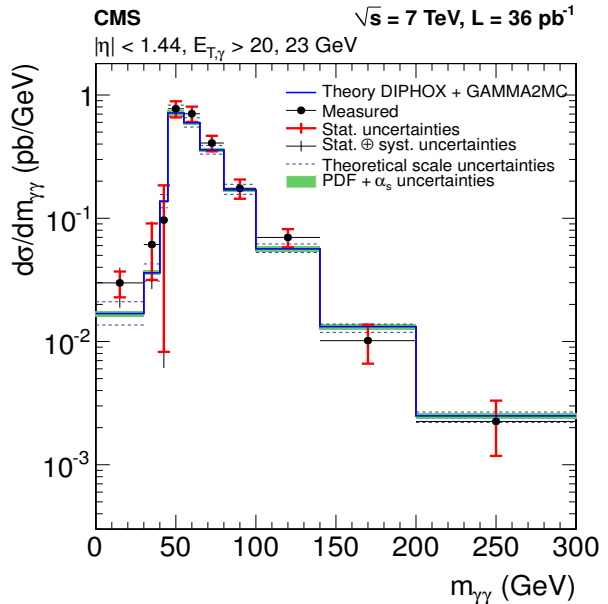


Figure 2: **Left:** Comparison between the ATLAS experimental cross sections and the predictions obtained with DIPHOX+GAMMA2MC (NLO) and 2gNNLO (NNLO) for the di-photon invariant mass<sup>20</sup>. The black dots correspond to data with error bars for their total uncertainties, which are dominated by the systematic component. The theoretical uncertainties include contributions from the limited size of the simulated sample, from the renormalization and factorization scales choice and from uncertainties on the parton distribution functions and on the hadronization and underlying event corrections. **Right:** Measured cross section of di-photon production as a function of the invariant mass of the photon pair for photons within the pseudorapidity region  $|\eta| < 1.44$ , as seen by CMS<sup>19</sup>. The inner and outer error bars on each point show the statistical and total experimental uncertainties. The 4% uncertainty on the integrated luminosity is not included in the error bars. The dotted line and shaded region represent the systematic uncertainties on the theoretical prediction from the theoretical scales and the PDFs, respectively.

## 6 Constraining parton distribution functions with photon measurements

Precise determination of the parton distribution functions (PDFs) of the proton is an essential input for phenomenological analyzes at the LHC. These PDFs are constrained using Deep Inelastic Scattering, jet production, Drell-Yan and W, Z production data. Photon data is usually not included, as large discrepancies between data and theories at fixed-target energies, greatly reduced their impact.

However, photon data is particularly sensitive to the gluon density, which is involved in a large fraction of the scattering processes at the LHC. As a matter of fact, gluon-gluon fusion is the dominant channel for the production of the SM Higgs boson, top-quark pairs or dijets, to mention a few. Recent studies<sup>23</sup> have shown that in the new energy range reached by the LHC, the isolated-photon theoretical prediction uncertainties are dominated by renormalization and factorization scales, away from non-perturbative effects due to the collinear fragmentation of final-state partons.

The impact of the available ATLAS and CMS photon and photon-jet measurements on the gluon density, was quantified in recent studies<sup>24,25</sup> using NLO theoretical calculations from the JETPHOX program combined with the NNPDF2.1 parton densities. The central value of the gluon distribution itself is unmodified but its uncertainty could be reduced by up to 20% around  $x \simeq 0.02$ . This lead to an uncertainty reduction of up to 20% for low mass Higgs production in the gluon-fusion channel.

## 7 Conclusion

ATLAS and CMS performed isolated-photon studies using the p-p collision data collected in 2010 and 2011. Both experiments have shown good agreement with theoretical calculations. Furthermore, the available isolated-photon data could also provide constraints on the gluon PDFs and thus on many relevant LHC processes, most importantly Higgs production in gluon-gluon fusion.

## References

1. P. Aurenche, R. Baier, M. Fontannaz, and D. Schiff, *Nucl. Phys. B* **297** (1988) 661.
2. P. Aurenche et al., *Phys. Rev. D* **39** (1989) 3275.
3. L. Evans and P. Bryant (editors) 2008 *JINST* **3** S08001.
4. ATLAS Collaboration, 2008 *JINST* **3** S08003.
5. CMS Collaboration, 2008 *JINST* **3** S08004.
6. ATLAS Collaboration, *Phys. Rev. D* **83**, (2011) 052005.
7. CMS Collaboration, *Phys. Rev. D* **84** (2011) 052011.
8. ATLAS Collaboration, *Phys. Lett. B* **706** (2011) 150.
9. ATLAS Collaboration, ATLAS-PHYS-PUB-2011-013, <http://cds.cern.ch/record/1395049>.
10. ATLAS Collaboration, ATLAS-CONF-2013-022, <http://cds.cern.ch/record/1525723>.
11. S. Catani, M. Fontannaz, J. Ph. Guillet and E. Pilon, *JHEP* **05** (2002) 028
12. T. Sjöstrand, S. Mrenna, and P. Z. Skands, *JHEP* **05** (2006) 026.
13. G. Corcella et al., *JHEP* **01** (2001) 010.
14. ATLAS Collaboration, *Phys. Rev. D* **85**, (2012) 092014.
15. ATLAS Collaboration, ATLAS-CONF-2013-023, <http://cds.cern.ch/record/1525728>.
16. CMS Collaboration, CMS-PAS-QCD-11-005, <http://cds.cern.ch/record/1525534>.
17. T. Gleisberg et al., *J. High Energy Phys.* **02** (2009) 007.
18. J. C. Collins and D. E. Soper, *Phys. Rev. D* **16**, (1977)2219 .
19. CMS Collaboration, *JHEP* **01** (2012) 133.
20. ATLAS Collaboration, *JHEP* **01** (2013) 086.
21. T. Binoth, J. Guillet, E. Pilon and M. Werlen, *Eur. Phys. J. C* **16** (2000) 311.
22. S. Catani et al., *Phys. Rev. Lett.* **108** (2012) 072001.
23. R. Ichou and D. d'Enterrria, *Phys. Rev. D* **82** (2010) 014015.
24. D. d'Enterrria and J. Rojo, *Nucl. Phys. B* **860** (2012) 311-338.
25. L. Carminati et al., *Europhysics Letters* **101** 61002 (2012).